Optimal Resource Allocation for Control of Networked Epidemic Models

Cameron Nowzari Victor M. Preciado George J. Pappas

Abstract

This work proposes and analyzes a generalized epidemic model over arbitrary directed graphs with heterogeneous nodes. The proposed model, called the *Generalized Susceptible-Exposed-Infected-Vigilant (G-SEIV)*, subsumes a large number of popular epidemic models considered in the literature as special cases. Using a mean-field approximation, we derive a set of ODEs describing the spreading dynamics, provide a careful analysis of the disease-free equilibrium, and derive necessary and sufficient conditions for global exponential stability. Building on this analysis, we consider the problem of containing an initial epidemic outbreak under budget constraints. More specifically, we consider a collection of control actions (e.g. administering vaccines/antidotes, limiting the traffic between cities, or running awareness campaigns), for which we are given suitable cost functions. In this context, we develop an optimization framework to provide solutions for the following two allocation problems: *(i)* find the minimum cost required to eradicate the disease at a desired exponential decay rate, and *(ii)* given a fixed budget, find the resource allocation to eradicate the disease at the fastest possible exponential decay rate. Our technical approach relies on the reformulation of these problems as geometric programs that can be solved efficiently in polynomial time using tools from graph theory and convex optimization. In contrast with previous works, our optimization framework allows us to simultaneously allocate different types of control resources over heterogeneous populations under budget constraints. We illustrate our results through numerical simulations.

I. Introduction

The analysis of spreading processes over complex networks has recently garnered a large amount of attention due to its relevance in a wide variety of practical applications. A few examples include epidemiology and public health [2], computer viruses [3], [4], and viral marketing [5]. Proper modeling and analysis of spreading processes is important in understanding the complex dynamics of these processes and in designing control strategies to tame (or promote) the spread. We propose a dynamic spreading model over networks that generalizes most epidemic models of current interest. In contrast with many existing models, we assume that the spreading takes place in an *arbitrary directed network of heterogeneous* nodes. These extensions allow our model to capture a wider variety of practical situations in which the interactions between nodes are not reciprocal, and nodes are not identical. After developing this dynamic model, we derive conditions for global exponential stability of the spreading process. Based on our stability analysis, we then propose an optimization framework to find the optimal allocation of control resources to contain a spreading process. We can numerically solve this allocation problem in polynomial time using geometric programming via standard off-the-shelf software.

A preliminary version of this work [1] was presented at the 2014 Conference on Decision and Control in Los Angeles, CA.

The authors are with the Department of Electrical and Systems Engineering, University of Pennsylvania, Philadelphia, PA, 19104, USA, {cnowzari,preciado,gjpappas}@seas.upenn.edu

Analysis of epidemic models has been a long standing research topic. The most widely studied spreading model in the literature is the Susceptible-Infected-Susceptible (SIS) model. Early works consider simplified versions of this model that assume each individual has equal contact to everyone else [2]. More general models were recently studied in [6] in the case of homogeneous mixing. The first paper, to our knowledge, that considered the situation of networked populations is [7]. Mean-field models over arbitrary contact graphs are now gaining popularity in both discrete-time [8] and continuous-time [9]. In [10], we find a detailed analysis of the SIS model in undirected networks of homogeneous agents. In this work, the authors derive conditions for global exponential stability of the disease-free equilibrium for both the continuous and discrete-time cases. If these conditions are not satisfied, the authors prove the existence of an endemic equilibrium where the disease never dies out. In practice, directed graphs may be more appropriate to model the spread of diseases in human populations with asymmetric contact rates, as well as the spread of computer viruses [3], [4], or information in social networks [11]. Similarly, by considering heterogeneous agents, we are able to capture the fact that individuals may respond to a given disease differently. This has been rigorously studied for the SIS model in [12].

Apart from analysis, the problem of controlling spreading processes in complex networks is also a thriving avenue for research. The majority of existing works consider the SIS model in different scenarios. Unlike works that propose suboptimal feedback control strategies such as [13], [14], we are interested in allocation strategies based on the spectral properties of appropriate matrices. In the control systems literature, Wan et al. proposed a method to design control strategies for the SIS model in directed networks using eigenvalue sensitivity analysis [15]. This is then formulated as a semidefinite programming problem in [16], and extended to a metapopulation model in [17], where nodes represent subpopulations (e.g. a city or district). A distributed approach to deciding the recovery parameters is presented in [18]. A game theoretic formulation of this problem is proposed in [19]. In [20], a multi-layer SIS model is considered where the spreading of multiple processes must be contained simultaneously. Most similar to our work is [21], in which a geometric programming allocation solution is proposed for the SIS model.

An interesting departure from the SIS model on arbitrary networks can be found in [22]. In this work, we find a Susceptible-Alert-Infected-Susceptible (SAIS) model where the alert state captures the effect of human awareness about the disease and its influence on the dynamics. Based on this model, an optimization framework to design cost-optimal disease awareness campaigns can be found in [23]. Unlike the above works, we utilize the analysis of our generalized epidemic model, G-SEIV, to formulate and solve optimal resource allocation problems that can be generalized to a large number of models including the SIS model. Furthermore, our framework allows us to simultaneously optimize the distribution of multiple types of control resources (e.g. vaccines, traffic constraints, and awareness campaigns).

The contributions of this paper are threefold.

1. We propose the continuous-time Generalized Susceptible-Exposed-Infected-Vigilant (G-SEIV) model in which both the exposed and infected states are infectious. This model generalizes many models studied in the literature including SIS, SIR, SIRS, SEIR, SEIV, SEIS, and SIV [24], [25]. Having two infectious states allows us to model human behavioral changes when infected with a disease. The exposed state corresponds to a person having the disease and being contagious, but not yet aware that they are sick. The infected state means a person is infected and aware of the disease, which means the person might behave differently. For instance, a person knowingly infected with a disease may have much less contact with others, yielding less chance of spreading the infection.

2. We use nonlinear analysis techniques to provide a useful coordinate change that allows us to study the stability of the spreading dynamics. By showing that the nonlinear system is upper-bounded by its linearization, we are able to provide necessary and sufficient conditions on the graph and parameters of the infection such that the disease dies out exponentially. Furthermore, this sets the stage for our third contribution.

3. We are interested in cost-optimal strategies for eradicating the disease. We consider three types of resources to control the disease: *(i) corrective resources* (e.g., antidotes to help increase recovery rates), *(ii) preventative resources* (e.g., vaccines to help increase resistance), and *(iii) preemptive resources* (e.g., awareness campaigns and/or limiting traffic to help reduce exposure to the disease). We assume that we have access to the cost functions associated with each control resource and show that, under mild conditions, we are able to find the optimal allocation of resources to eradicate the disease. We illustrate our results through numerical simulations on synthetic data.

The structure of the paper is as follows. The description of the G-SEIV model is formally presented in Section II. We state the main problems of interest in Section III and show how they can be reformulated as geometric programs in Section IV. We illustrate our results through simulations in Section V and finish with closing remarks in Section VI.

Notation and Preliminaries

We denote by $\mathbb{R}$, $\mathbb{R}_{\geq 0}$, and $\mathbb{R}_{>0}$ the sets of real, nonnegative real, and positive real numbers, respectively. Given $m_1, \ldots, m_N$ where $m_i \in$, we let $\operatorname{diag}(m_1, \ldots, m_N)$ denote the $N \times N$ diagonal matrix with $m_1, \ldots, m_N$ on the diagonal. We define the indicator function $\mathbf{1}_Z$ to be 1 if Z is true, and 0 otherwise. Given two column vectors $\mathbf{x}, \mathbf{y} \in \mathbb{R}^N$, we let $\mathbf{xy}$ denote their Hadamard product, i.e, $\mathbf{xy} = (x_1 y_1, \ldots, x_N y_N)^T$.

A *directed* graph (also called digraph) is defined as $\mathcal{G} \triangleq (\mathcal{V}, \mathcal{E})$, where $\mathcal{V} \triangleq \{v_1, \ldots, v_N\}$ is a set of N nodes and $\mathcal{E} \subseteq \mathcal{V} \times \mathcal{V}$ is a set of ordered pairs of nodes called directed edges. By convention, we say that (v_j, v_i) is an edge from v_j pointing towards v_i. We define the in-neighborhood of node v_i as $\mathcal{N}_i^{in} \triangleq \{j : (v_j, v_i) \in \mathcal{E}\}$, i.e., the set of nodes with edges pointing towards v_i. A directed path from v_{i_1} to v_{i_l} in $\mathcal{G}$ is an ordered set of vertices $(v_{i_1}, v_{i_2}, \ldots, v_{i_l})$ such that $\left(v_{i_s}, v_{i_{s+1}}\right) \in \mathcal{E}$ for $s = 1, \ldots, l-1$. A directed graph $\mathcal{G}$ is *strongly connected* if, for every pair of nodes $v_i, v_j \in \mathcal{V}$, there is a directed path from v_i to v_j.

The *adjacency matrix* of a digraph $\mathcal{G}$, denoted by $A_{\mathcal{G}} = [a_{ij}]$, is an $N \times N$ matrix defined entry-wise as $a_{ij} = 1$ if edge $(v_j, v_i) \in \mathcal{E}$, and $a_{ij} = 0$ otherwise. The matrix $A_{\mathcal{G}}$ is *irreducible* if and only if its associated graph $\mathcal{G}$ is strongly connected. For simplicity, we only consider unweighted digraphs in this paper but note that all results trivially hold for all positively weighted digraphs as well.

Given a matrix $M \in \mathbb{R}^{N \times N}$, we denote its eigenvectors and corresponding eigenvalues by $\mathbf{v}_1(M), \ldots, \mathbf{v}_N(M)$ and $\lambda_1(M), \ldots, \lambda_N(M)$, respectively, where we order them in decreasing order of their real parts, i.e., $\Re(\lambda_1) \geq \Re(\lambda_2) \geq \ldots \geq \Re(\lambda_N)$. We call $\lambda_1(M)$ and $\mathbf{v}_1(M)$ the dominant eigenvalue and eigenvector of M, respectively. The spectral radius of M, denoted by $\rho(M)$, is the maximum modulus across all eigenvalues of M.

II. Model description

Our model follows the idea of the N-intertwined SIS model in [9]. The model we study, called the Generalized Susceptible-Exposed-Infected-Vigilant model (G-SEIV), is described as follows. Consider a virus spreading model where each node can be in one of four states: Susceptible $\mathbb{S}$, Exposed $\mathbb{E}$, Infected $\mathbb{I}$, or Vigilant $\mathbb{V}$. The susceptible state $\mathbb{S}$ corresponds to a healthy node. The exposed state $\mathbb{E}$ corresponds to a node that has been exposed to the disease and is contagious, but is not aware of the contagion (e.g. the symptoms have not yet been developed). The infected state $\mathbb{I}$ corresponds to an infected node that is aware of the infection (e.g. the node is symptomatic). Finally, the vigilant state $\mathbb{V}$ corresponds to a node that is not contaminated, but is also not immediately susceptible to the virus (e.g. vaccinated, quarantined, or recently recovered).

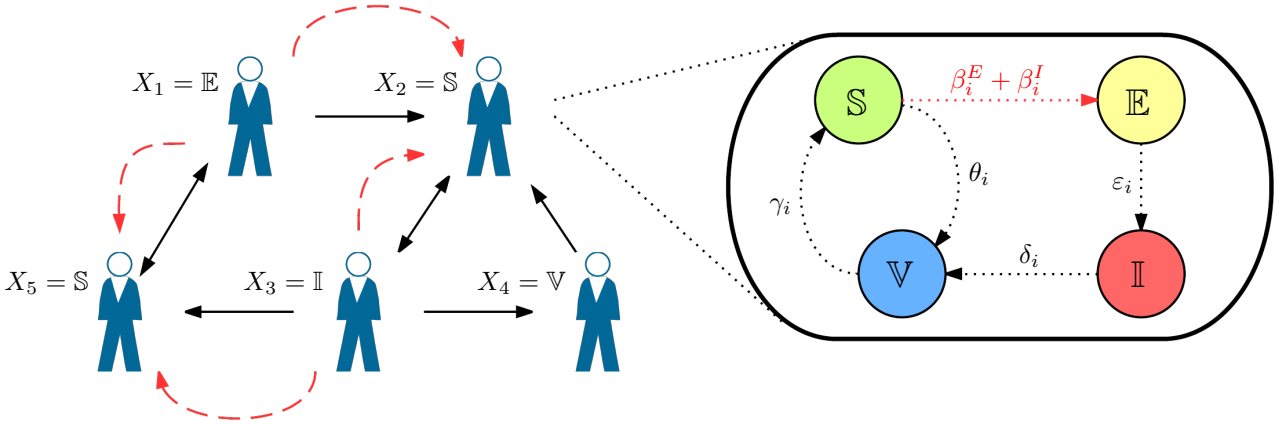

Fig. 1. An example of a five node network (left) with underlying directed contact graph shown by solid black lines and effects of infection shown by dashed red lines and the stochastic compartmental model (right) for node $i = 2$ with one exposed and infected in-neighbor.

For each node $i \in \{1, \dots, N\}$ we define the random variable $X_i(t) \in \{\mathbb{S}, \mathbb{E}, \mathbb{I}, \mathbb{V}\}$ as the state of node i at a given time t. A susceptible node is only able to become exposed if it has at least one neighbor that is either exposed or infected on a contact graph $\mathcal{G}$. We assume that $\mathcal{G}$ is strongly connected. Figure II (left) shows a simple five node network with underlying digraph $\mathcal{G}$ shown with solid black lines. The dashed red arrows indicate the potential paths of infection in the graph (notice that the 'tails' of those arrows are either infected or exposed, and the 'heads' are susceptible). As discussed above, a node i can only be affected by a neighboring $j \in \mathcal{N}_i^{\text{in}}$ if j is in either the exposed state $\mathbb{E}$ or infected state $\mathbb{I}$ and i is in the susceptible state $\mathbb{S}$.

The stochastic dynamics of each nodal state is described as a networked Markov process, similar to the one proposed in [9], but extended to the case of four states per node. The transition between states is graphically represented in Fig. II (right) for node X_2. The parameter δ_i in Fig. II represents the natural recovery rate of node i when infected, i.e., the rate at which infected states transition into the vigilant state. The parameter γ_i is the rate of becoming susceptible after the node has become vigilant. This could represent, for example, the rate at which the immune system of an individual that has recovered from a disease (e.g., the flu) becomes susceptible to a new infection. Similarly, β_i^E (resp. $\beta_i^I \leq \beta_i^E$) corresponds to the natural rate at which a susceptible nodes i transitions to the exposed state due to contact with a node in the exposed state (resp. infected state). Let ε_i be the rate at which an exposed node i becomes infected, (the rate at which an exposed individual exhibits symptoms). Finally, let θ_i be the rate at which a susceptible node i becomes vigilant (e.g. through vaccination or quarantine).

The dynamics of the epidemic spread is then modeled using a networked Markov process with the following transition rates, for a chosen timestep Δt [26]:

$$\begin{aligned}
P(X_i(t') = \mathbb{E} | X_i(t) = \mathbb{S}, X(t)) &= \beta_i^E \Delta t Y_i(t) + \beta_i^I \Delta t Z_i(t) + o(\Delta t), \\
P(X_i(t') = \mathbb{V} | X_i(t) = \mathbb{S}, X(t)) &= \theta_i \Delta t + o(\Delta t), \\
P(X_i(t') = \mathbb{I} | X_i(t) = \mathbb{E}, X(t)) &= \varepsilon_i \Delta t + o(\Delta t), \\
P(X_i(t') = \mathbb{V} | X_i(t) = \mathbb{I}, X(t)) &= \delta_i \Delta t + o(\Delta t), \\
P(X_i(t') = \mathbb{S} | X_i(t) = \mathbb{V}, X(t)) &= \gamma_i \Delta t + o(\Delta t),
\end{aligned} \tag{1}$$

where $t' = t + \Delta t$, and

$$Y_i(t) \triangleq \sum_{j \in \mathcal{N}_i^{\text{in}}} \mathbf{1}_{X_j(t) = \mathbb{E}}, \quad Z_i(t) \triangleq \sum_{j \in \mathcal{N}_i^{\text{in}}} \mathbf{1}_{X_j(t) = \mathbb{I}},$$

are the number of exposed and infected in-neighbors of node i, respectively.

Fig. II (right) shows the stochastic compartmental model for node 2, which is affected by one exposed and one infected node as shown on the left. In this figure the solid black lines show the internal state transitions and the dashed red line corresponds to the node having one or more infected or exposed neighbors.

According to the Markov process described in (1), the whole network state $X(t)$ lives in a 4^N dimensional space. The exponential size of the state space makes the Markov process very hard to analyze. Instead, we consider a mean-field approximation, similar to the one proposed in [9], that allows us to study the dynamics of the spreading using a set of $3N$ nonlinear ODEs (we refer the reader to [9] for a detailed derivation of the mean-field approximation for the SIS model; and to [27] for a numerical exploration of mean-field approximations in networked dynamics). We denote by $\left[p_i^S(t), p_i^E(t), p_i^I(t), p_i^V(t)\right]^T$ the probability vector associated with node i being in each of the states $\mathbb{S}, \mathbb{E}, \mathbb{I}, \mathbb{V}$, respectively, i.e.,

$$\begin{aligned}
p_i^S(t) + p_i^E(t) + p_i^I(t) + p_i^V(t) &= 1, \\
p_i^S(t), p_i^E(t), p_i^I(t), p_i^V(t) &\geq 0,
\end{aligned} \tag{2}$$

for all $i \in \{1, \ldots, N\}$ and $t \in \mathbb{R}_{\geq 0}$. For simplicity, we drop the explicit dependence on time when it is not important. The mean-field approximation of the G-SEIV model is then given by

$$\begin{aligned}
\dot{p}_i^S &= \gamma_i p_i^V - \theta_i p_i^S - p_i^S \Big(\sum_{j \in \mathcal{N}_i^{\text{in}}} \beta_i^E p_j^E + \beta_i^I p_j^I \Big), \\
\dot{p}_i^E &= p_i^S \Big(\sum_{j \in \mathcal{N}_i^{\text{in}}} \beta_i^E p_j^E + \beta_i^I p_j^I \Big) - \varepsilon_i p_i^E, \\
\dot{p}_i^I &= \varepsilon_i p_i^E - \delta_i p_i^I, \\
\dot{p}_i^V &= \delta_i p_i^I + \theta_i p_i^S - \gamma_i p_i^V,
\end{aligned} \tag{3}$$

for all $i \in \{1, \ldots, N\}$. From (2), we see that one of the states is redundant, reducing the entire network state to be in $\mathbb{R}_{\geq 0}^{3N}$.

Remark II.1 (Relation between Markov process and mean-field approximation) The remainder of this paper is focused on the analysis and control of the deterministic mean-field approximation. Based upon extensive simulations, we conjecture that the exposed and infected states of our approximation upper-bound the expectations of these states in the original stochastic

model. This is known to be true for the SIS model [28], [29], [30] and very recently shown to be true for a more general SIRS model [31]. Given the rigor required to properly justify this claim, we leave this to be addressed in future works. •

III. Problem formulation

Given the G-SEIV model developed in Section II, we are now ready to state the two main problems we seek to solve. The first problem, which we denote the *budget-constrained allocation problem*, consists of optimizing the rate of decay to the disease-free equilibrium given a fixed budget to invest on various control resources. The second problem, denoted the *rate-constrained allocation problem*, consists of minimizing the cost of eradicating a disease at a desired rate of decay. In both control problems, we consider three types of protection resources: *(i)* corrective resources (e.g. antidotes) able to increase the recovery rate δ_i of the node to which they are allocated, *(ii)* preventative resources (e.g. vaccines) able to increase the parameter θ_i, and *(iii)* preemptive resources able to decrease the values of the infection rates β_i^E and β_i^I of the node to which they are allocated. For example, a preemptive resource can be the restriction of incoming traffic to a particular city. We assume that we are able to modify these parameters within some feasible bounds

$$\begin{aligned} 0 < \underline{\theta}_i \leq \theta_i \leq \overline{\theta}_i, \qquad & 0 < \underline{\delta}_i \leq \delta_i \leq \overline{\delta}_i, \\ 0 < \underline{\beta}_i^E \leq \beta_i^E \leq \overline{\beta}_i^E, \qquad & 0 < \underline{\beta}_i^I \leq \beta_i^I \leq \overline{\beta}_i^I. \end{aligned} \tag{4}$$

We define four cost functions to account for the cost of controlling each one of the variables $\theta_i, \delta_i, \beta_i^E$, and β_i^I. The preventative cost function $f_i(\theta_i)$ accounts for the cost of tuning the value of θ_i of node i. We assume that this cost function is monotonically increasing since investing in a node should increase its rate θ_i of becoming vigilant. Furthermore, we assume that $\underline{\theta}_i$ is the lowest achievable value for the parameter θ_i. In practice, it is sensible to assume that this value is achieved in the absence of any investment to tune θ_i; therefore, $f_i(\underline{\theta}_i) = 0$ for all i. Following a similar logic, we can assume that the corrective cost function $g_i(\delta_i)$ is a monotonically increasing function, while the preemptive costs $h_i^E(\beta_i^E)$ and $h_i^I(\beta_i^I)$ are monotonically decreasing. Also, in the absence of investment we have that $f_i(\underline{\theta}_i) = g_i(\underline{\delta}_i) = h_i^E(\overline{\beta}_i^E) = h_i^I(\overline{\beta}_i^I) = 0$ for all i. We let $\varepsilon_i, \gamma_i > 0$ be fixed parameters that depend on the nature of the disease and each individual node. In other words, the rate at which a node develops symptoms (represented by ε_i) is a variable that is hard to control in practice; hence, we assume it to be fixed. Similarly, the rate in which an individual that has recently recovered from a disease (e.g. the flu) can get infected again is also hard to control in practice. In the next section, we analyze the disease-free equilibria of the G-SEIV model.

A. Analysis of disease-free equilibria

We are interested in studying the disease-free equilibrium of (3). At this equilibrium point, we have that $p_i^{E^*} = p_i^{I^*} = 0$. Note that in the disease-free equilibrium the healthy states p_i^S, p_i^V are not necessarily 0, and their equilibrium values depend on the parameters θ_i and γ_i. In what follows, we compute the values of the healthy states at the disease free equilibrium.

Since $p_i^S = 1 - p_i^E - p_i^I - p_i^V$, we can reduce the system of $4N$ differential equations in (3) to $3N$ equations

$$\begin{aligned} \dot{p}_i^E &= (1 - p_i^E - p_i^I - p_i^V)\Big(\sum_{j \in \mathcal{N}_i^{\text{in}}} \beta_i^E p_j^E + \beta_i^I p_j^I \Big) - \varepsilon_i p_i^E, \\ \dot{p}_i^I &= \varepsilon_i p_i^E - \delta_i p_i^I, \\ \dot{p}_i^V &= \delta_i p_i^I + \theta_i (1 - p_i^E - p_i^I - p_i^V) - \gamma_i p_i^V(t), \end{aligned} \tag{5}$$

for all $i \in \{1, \ldots, N\}$. We find the disease-free equilibrium point $p_i^{V^*}$ from the last equation in (5), by substituting $\dot{p}_i^V = 0$ and $p_i^{E^*} = p_i^{I^*} = 0$ to be

$$p_i^{V^*} = \frac{\theta_i}{\theta_i + \gamma_i}.$$

Notice that, at this equilibrium, $p_i^{S^*} = 1 - p_i^{V^*}$.

The following proposition states a spectral condition to converge towards the disease-free equilibrium exponentially fast, i.e., eradicate the disease at an exponential rate. In the statement of this proposition, it will be useful to resort to the following vectors of parameters $\beta^E \triangleq (\beta_1^E, \ldots, \beta_N^E)$, $\beta^I \triangleq (\beta_1^I, \ldots, \beta_N^I)$, $\delta \triangleq (\delta_1, \ldots, \delta_N)$, $\varepsilon \triangleq (\varepsilon_1, \ldots, \varepsilon_N)$, $\gamma \triangleq (\gamma_1, \ldots, \gamma_N)$, and $\theta \triangleq (\theta_1, \ldots, \theta_N)$:

Proposition III.1 *Consider the G-SEIV epidemic model in* (3) *and assume that all the parameters in* (4) *are strictly positive. Define the matrix*

$$Q = \begin{bmatrix} TB^E A_{\mathcal{G}} - E & TB^I A_{\mathcal{G}} \\ E & -D \end{bmatrix}, \tag{6}$$

where $A_{\mathcal{G}}$ is the adjacency matrix of the strongly connected contact graph $\mathcal{G}$, $B^E \triangleq \operatorname{diag}\left(\beta^E\right), B^I \triangleq \operatorname{diag}\left(\beta^I\right), D \triangleq \operatorname{diag}\left(\delta\right), E \triangleq \operatorname{diag}\left(\varepsilon\right), T \triangleq \operatorname{diag}\left(\frac{\gamma}{\theta+\gamma}\right)$. Then, the largest real part of the eigenvalues of Q satisfies

$$\lambda_1(Q) \leq -k \tag{7}$$

for some $k > 0$ if and only if the disease-free equilibrium is globally exponentially stable with an exponential decay rate upper bounded by k.

Proof: In the Appendix. ■

Remark III.2 (Tightness of convergence rate bound) It is important to note that although Proposition III.1 only provides an upper bound on the exponential convergence rate of the nonlinear system, this bound is tight. This can be shown by seeing that although the nonlinear terms are all helpful (in terms of speeding up the convergence), they are all sums of second order monomials. This means that the nonlinear terms go to 0 much faster than the linear terms as the state of the system approaches the disease-free equilibrium.

Based on Proposition III.1, we now formulate the two main problems considered in our work. In both problems, a central decision maker (e.g. a health agency) is responsible for allocation a variety of control resources to contain an epidemic outbreak. As mentioned above, we assume that we can invest resources to tune the parameters θ, δ, β^E, and β^I, within the feasible ranges defined in (4). For simplicity of notation, we define the global set of parameters as $\mathcal{P} \triangleq \{\theta, \delta, \beta^E, \beta^I\}$. The budget-constrained allocation problem is formalized next.

Problem III.3 (Budget-constrained allocation) Given a fixed budget $C > 0$, find the cost-optimal allocation of resources to

eradicate the disease at the maximum possible exponential decay rate. This problem can be mathematically formulated as

$$\begin{aligned} \min_{\mathcal{P}} \quad & \lambda_1(Q) \\ \text{s.t.} \quad & \textstyle\sum_{j=1}^{N} f_j(\theta_j) + g_j(\delta_j) + h_j^E(\beta_j^E) + h_j^I(\beta_j^I) \leq C, \\ & (\underline{\beta}_i^E, \underline{\beta}_i^I) \leq (\beta_i^E, \beta_i^I) \leq (\overline{\beta}_i^E, \overline{\beta}_i^I), \\ & (\underline{\theta}_i, \underline{\delta}_i) \leq (\theta_i, \delta_i) \leq (\overline{\theta}_i, \overline{\delta}_i), \end{aligned}$$

for all $i \in \{1, \ldots, N\}$. The first constraint in the above optimization program accounts for the budget constraint, while the second and third constraints represents the range in which the control parameters can be tuned.

In the problem above, the decision maker is given a fixed budget to be invested in resources to eradicate the disease at the fastest possible decay rate. However, this budget may not be sufficient to eradicate the disease. It may be the case that the optimal decay rate in the budget-constraint allocation problem is negative (i.e., the disease never dies out). Therefore, it is of interest to find the minimum budget required to eradicate the disease at a desired exponential decay rate. The rate-constrained allocation problem is formalized next.

Problem III.4 (Rate-constrained allocation) Given a desired decay rate $k > 0$, find the cost-optimal allocation of resources to eradicate the disease with exponential decay rate greater than or equal to k. This problem can be mathematically formulated as

$$\begin{aligned} \min_{\mathcal{P}} \quad & \textstyle\sum_{j=1}^{N} f_j(\theta_j) + g_j(\delta_j) + h_j^E(\beta_j^E) + h_j^I(\beta_j^I) \\ \text{s.t.} \quad & \lambda_1(Q) \leq -k, \\ & (\underline{\beta}_i^E, \underline{\beta}_i^I) \leq (\beta_i^E, \beta_i^I) \leq (\overline{\beta}_i^E, \overline{\beta}_i^I), \\ & (\underline{\theta}_i, \underline{\delta}_i) \leq (\theta_i, \delta_i) \leq (\overline{\theta}_i, \overline{\delta}_i), \end{aligned}$$

for all $i \in \{1, \ldots, N\}$.

As a particular case of Problem III.4, we may want to find the minimum budget C^* needed for $\mathcal{Q}$ to be Hurwitz. In other words, C^* is the minimum budget required by the health agency to be able to eradicate the disease. Due to the practical importance of this particular case, we state it below for future reference.

Problem III.5 (Eradication allocation) Find the minimum budget (and its allocation) required to ensure eradication of the disease. This can mathematically formulated as:

$$\begin{aligned} \min_{\mathcal{P}} \quad & \textstyle\sum_{i=j}^{N} f_j(\theta_j) + g_j(\delta_j) + h_j^E(\beta_j^E) + h_j^I(\beta_j^I) \\ \text{s.t.} \quad & \lambda_1(Q) < 0, \\ & (\underline{\beta}_i^E, \underline{\beta}_i^I) \leq (\beta_i^E, \beta_i^I) \leq (\overline{\beta}_i^E, \overline{\beta}_i^I), \\ & (\underline{\theta}_i, \underline{\delta}_i) \leq (\theta_i, \delta_i) \leq (\overline{\theta}_i, \overline{\delta}_i), \end{aligned}$$

for all $i \in \{1, \ldots, N\}$.

In the following section we propose an approach to solve these problems in polynomial time under certain assumptions on the cost functions.

IV. A CONVEX OPTIMIZATION FRAMEWORK

In this section we show how the problems presented in Section III can be efficiently solved by recasting them as equivalent geometric programs [32]. Geometric programs are quasiconvex optimization problems that can be transformed into a convex problem using a logarithmic change of variables and efficiently solved using off-the-shelf software in polynomial time [32], [33].

A. Geometric programming

We begin by briefly reviewing some important concepts that will be useful in our derivations. Let $\mathbf{x} = (x_1, \ldots, x_N)^T$, where $x_1, \ldots, x_N > 0$ denote N decision variables. In the context of geometric programs, a *monomial* function $h(\mathbf{x})$ is a real-valued function of the form $h(\mathbf{x}) = c_0 x_1^{a_1} x_2^{a_2} \ldots x_N^{a_N}$ with $c_0 > 0$ and $a_i \in \mathbb{R}$ for all $i \in \{1, \ldots, N\}$. A *posynomial* function $q(\mathbf{x})$ is a real-valued function that is a sum of monomials, i.e., $q(\mathbf{x}) = \sum_{k=1}^{K} c_k x_1^{a_{1,k}} x_2^{a_{2,k}} \ldots x_N^{a_{N,k}}$, where $c_k > 0$ and $a_{i,k} \in \mathbb{R}$ for all $i \in \{1, \ldots, N\}$ and $k \in \{1, \ldots, K\}$.

A geometric program (GP) is an optimization problem of the form

$$\begin{aligned} \underset{\mathbf{x}}{\text{minimize}} \quad & f(\mathbf{x}) \\ \text{such that} \quad & q_i(\mathbf{x}) \leq 1, \; i = 1, \ldots, m, \\ & h_j(\mathbf{x}) = 1, \; j = 1, \ldots, p, \end{aligned} \tag{8}$$

where f and q_i are posynomial functions, and h_j are monomial functions. A GP is a quasiconvex optimization problem [32] that can be transformed to a convex problem via a logarithmic change of variables $y_i = \log x_i$, and a logarithmic transformation of the objective and constraint functions (for more details about this transformation, see [33]).

We are now interested in reformulating Problems III.3, III.4, and III.5 in the form (8). This requires mild assumptions on the cost functions to ensure all constraints can be written in terms of posynomials and monomials. Posynomial functions can be used to fit any function that is convex in log-log scale with arbitrary accuracy. Furthermore, there are well-developed numerical methods to fit posynomials to real data. For more details about the modeling abilities of posynomial, we refer the reader to [33, Section 8]. In the following section, we recast the problems posed in Section III as standard GPs.

B. Optimal resource allocation

In our derivations, it will be useful to resort to the following result from [32, Chapter 4].

Proposition IV.1 *Consider an $N \times N$ nonnegative, irreducible matrix $M(\mathbf{x})$ with entries being either 0 or posynomials with domain $\mathbf{x} \in \mathcal{S}$ where $\mathcal{S} = \cap_{i=1}^{m} \{\mathbf{x} \in \mathbb{R}^k_{>0} \mid f_i(\mathbf{x}) \leq 1\}$ for some posynomials f_i. Then, minimizing the largest real part of the eigenvalues of $M(\mathbf{x})$, denoted by $\lambda_1(M(\mathbf{x}))$, over $\mathbf{x} \in \mathcal{S}$ is equivalent to solving the following GP:*

$$\begin{aligned} \underset{\lambda, \{u_i\}_{i=1}^N, \mathbf{x}}{\text{minimize}} \quad & \lambda \\ \text{such that} \quad & \frac{\sum_{j=1}^{N} M_{ij}(\mathbf{x}) u_j}{\lambda u_i} \leq 1, \quad i \in \{1, \ldots, N\}, \\ & f_i(\mathbf{x}) \leq 1, \qquad\quad i \in \{1, \ldots, m\}. \end{aligned} \tag{9}$$

Remark IV.2 The value of the argument λ that minimizes (9) is equal to the minimum value of the largest real part of the eigenvalues of $M(\mathbf{x})$. As a result of the Perron-Frobenius theorem we know there exists a corresponding eigenvector with components that are all strictly positive allowing us to write this as a GP. Notice that the numerator on the left-hand side of the first constraint in (9) is a posynomial, while the denominator is a monomial. Since the division of a posynomial by a monomial results in a posynomial function, the optimization in (9) is a standard GP as described in (8).

In what follows, we shall use Proposition IV.1 to minimize the largest real part of the eigenvalues of the matrix Q in (7), which according to Proposition III.1 determines an upper bound on the exponential decay rate of the spreading. Unfortunately, the matrix Q does not satisfy the requirements of Proposition (IV.1) since it is not nonnegative. We can address this issue by creating a nonnegative matrix from Q by simply adding a constant $\phi \triangleq \max\{\varepsilon_i, \overline{\delta}_i\}_{i=1}^N$ to the diagonal. We then obtain

$$\overline{Q} \triangleq \begin{bmatrix} TB^E A_{\mathcal{G}} + \widetilde{E} & TB^I A_{\mathcal{G}} \\ E & \widetilde{D} \end{bmatrix}, \tag{10}$$

where $\widetilde{E} = \text{diag}(\{\widetilde{\varepsilon}_i\}) = \phi\mathbf{I} - E \geq 0$ and $\widetilde{D} = \text{diag}(\{\widetilde{\delta}_i\}) = \phi\mathbf{I} - D \geq 0$. Notice that the eigenvalues of $\overline{Q}$ are equal to the eigenvalues of Q plus the known quantity ϕ.

In what follows, we show how to solve Problem III.3 by applying Proposition IV.1 over $\overline{Q}$. In particular, we show that this problem can be efficiently solved as a GP if the cost functions f_i and g_i satisfy the following assumption.

Assumption 1 *The cost functions f_i and g_i can be written as*

$$f_i(\theta_i) = \widetilde{f}_i\left(\frac{\gamma_i}{\theta_i + \gamma_i}\right), \tag{11}$$

$$g_i(\delta_i) = \widetilde{g}_i\left(\phi - \delta_i\right), \tag{12}$$

where $\widetilde{f}_i$ and $\widetilde{g}_i$ are posynomial functions with domains $\widetilde{f}_i : \left[\gamma_i/(\overline{\theta}_i + \gamma_i), \gamma_i/(\underline{\theta}_i + \gamma_i)\right] \to [f(\underline{\theta}_i), f(\overline{\theta}_i)]$ and $\widetilde{g}_i : \left[\phi - \overline{\delta}_i, \phi - \underline{\delta}_i\right] \to \left[g(\underline{\delta}_i), g(\overline{\delta}_i)\right]$.

Theorem IV.3 (Solution to the budget-constrained problem) *Under Assumption 1, Problem III.3 can be solved by solving the following auxiliary geometric program with decision variables $\lambda, \left\{\beta_i^I, \beta_i^E, \widetilde{\delta}_i, \tau_i, u_i, v_i\right\}_{i=1}^N$:*

$$\begin{aligned} \text{min.} \quad & \lambda \\ \text{s.t.} \quad & \textstyle\sum_{j=1}^N a_{ij}\tau_i\left(\beta_i^E u_j + \beta_i^I v_j\right) + (\phi - \varepsilon_i)u_i \leq \lambda u_i, \\ & \varepsilon_i u_i + \widetilde{\delta}_i v_i \leq \lambda v_i, \\ & \textstyle\sum_{j=1}^N h_j^I\left(\beta_j^I\right) + h_j^E\left(\beta_j^E\right) + \widetilde{g}_j\left(\widetilde{\delta}_j\right) + \widetilde{f}_j\left(\tau_j\right) \leq C, \\ & \frac{\gamma_i}{\overline{\theta}_i + \gamma_i} \leq \tau_i \leq \frac{\gamma_i}{\underline{\theta}_i + \gamma_i}, \\ & \phi - \overline{\delta}_i \leq \widetilde{\delta}_i \leq \phi - \underline{\delta}_i, \\ & \left(\underline{\beta}_i^I, \underline{\beta}_i^E\right) \leq \left(\beta_i^I, \beta_i^E\right) \leq \left(\overline{\beta}_i^I, \overline{\beta}_i^E\right), \end{aligned} \tag{13}$$

for all $i \in \{1, \ldots, N\}$, where $\delta_i^* = \phi - \widetilde{\delta}_i^*$ and $\theta_i^* = \frac{\gamma_i(1-\tau_i^*)}{\tau_i^*}$ solves the problem with rate $\lambda_1(Q) \leq \lambda^* - \phi$.

Proof: As we mentioned above, solving Problem III.3 is equivalent to minimizing the maximum eigenvalue of $\overline{Q}$ under budget constraints. According to Proposition IV.1, we can minimize the maximum eigenvalue of $\overline{Q}$ by solving the following

GP with decision variables $\lambda, \mathcal{P}, \{u_i, v_i\}_{i=1}^N$:

$$\begin{aligned} \text{min,} \quad & \lambda \\ \text{s.t.} \quad & \overline{Q} \begin{bmatrix} \mathbf{u} \\ \mathbf{v} \end{bmatrix} \leq \lambda \begin{bmatrix} \mathbf{u} \\ \mathbf{v} \end{bmatrix}, \\ & \textstyle\sum_{i=1}^N h_i^I\left(\beta_i^I\right) + h_i^E\left(\beta_i^E\right) + g_i\left(\delta_i\right) + f_i\left(\theta_i\right) \leq C, \\ & (\underline{\beta}_i^E, \underline{\beta}_i^I) \leq (\beta_i^E, \beta_i^I) \leq (\overline{\beta}_i^E, \overline{\beta}_i^I), \\ & (\underline{\theta}_i, \underline{\delta}_i) \leq (\theta_i, \delta_i) \leq (\overline{\theta}_i, \overline{\delta}_i), \end{aligned} \tag{14}$$

for all $i \in \{1, \ldots, N\}$. Notice that $\overline{Q}$ is irreducible when $A_{\mathcal{G}}$ is the adjacency matrix of a strongly connected graph $\mathcal{G}$ and $\varepsilon_i, \delta_i > 0$ for all i. The first constraint in (14) can be split into the following two constraints:

$$\begin{aligned} \frac{\gamma_i}{\theta_i + \gamma_i} \sum_{j=1}^N a_{ij}\left(\beta_i^E u_j + \beta_i^I v_j\right) + (\phi - \varepsilon_i)u_i &\leq \lambda u_i, \\ \varepsilon_i u_i + (\phi - \delta_i)v_i &\leq \lambda v_i, \end{aligned}$$

for $i \in \{1, \ldots, N\}$. In order to rewrite the above constraints as posynomial constraints, we define the variables $\tau_i \triangleq \gamma_i / (\theta_i + \gamma_i)$ and $\widetilde{\delta}_i \triangleq \phi - \delta_i$, which results in

$$\begin{aligned} \sum_{j=1}^N a_{ij}\tau_i\left(\beta_i^E u_j + \beta_i^I v_j\right) + (\phi - \varepsilon_i)u_i &\leq \lambda u_i, \\ \varepsilon_i u_i + \widetilde{\delta}_i v_i &\leq \lambda v_i. \end{aligned}$$

Notice that, due to the definition of ϕ, both $\phi - \varepsilon_i$ and $\phi - \delta_i$ are nonnegative for all i. After the above change of variables, we now seek to optimize over the new decision variables τ_i and $\widetilde{\delta}_i$ rather than θ_i and δ_i in their respective domains. It is easy to verify that the box constraints in (13) ensure that the new decision variables are in the correct domains. Furthermore, due to Assumption 1, the problem (13) is now written in the standard GP form (8). Finally, noticing that $\lambda_1(\overline{Q}) = \lambda_1(Q) + \phi$ concludes the proof. ■

Remark IV.4 Theorem IV.3 allows us to find the joint optimal allocation of heterogeneous resources in a networked population under a budget constraint. We do this by exactly transforming the original problem III.3 into a GP by using an appropriate change of variables.

We are able to solve Problem III.4 in a similar fashion as stated next.

Theorem IV.5 (Solution to rate-constrained problem) *Under Assumption 1, Problem III.4 can be solved by solving the following auxiliary geometric program with decision variables* $\left\{\beta_i^I, \beta_i^E, \widetilde{\delta}_i, \tau_i, u_i, v_i\right\}_{i=1}^N$*:*

$$\begin{aligned} \text{min.} \quad & \textstyle\sum_{j=1}^N h_j^I\left(\beta_j^I\right) + h_j^E\left(\beta_j^E\right) + \widetilde{g}_j\left(\widetilde{\delta}_j\right) + \widetilde{f}_j\left(\tau_j\right) \\ \text{s.t.} \quad & \textstyle\sum_{j=1}^N a_{ij}\tau_i\left(\beta_i^E u_j + \beta_i^I v_j\right) + (\phi - \varepsilon_i)u_i \leq (\phi - k)u_i, \\ & \varepsilon_i u_i + \widetilde{\delta}_i v_i \leq (\phi - k)v_i, \\ & \frac{\underline{\gamma}_i}{\overline{\theta}_i + \gamma_i} \leq \tau_i \leq \frac{\gamma_i}{\underline{\theta}_i + \gamma_i}, \\ & \phi - \overline{\delta}_i \leq \widetilde{\delta}_i \leq \phi - \underline{\delta}_i, \\ & \left(\underline{\beta}_i^I, \underline{\beta}_i^E\right) \leq \left(\beta_i^I, \beta_i^E\right) \leq \left(\overline{\beta}_i^I, \overline{\beta}_i^E\right), \end{aligned} \tag{15}$$

for all $i \in \{1, \dots, N\}$, *where* $\delta_i^* = \phi - \widetilde{\delta}_i^*$ *and* $\theta_i^* = \frac{\gamma_i(1-\tau_i^*)}{\tau_i^*}$ *solves the problem with cost*

$$\sum_{i=1}^{N} h_i^I(\beta_i^{I^*}) + h_i^E(\beta_i^{E^*}) + g_i(\delta_i^*) + f_i(\theta_i^*).$$

Proof: The proof of this Theorem follows similar steps as those in the proof of Theorem IV.3. ■

Problem III.5 is a particular case of Problem III.4 in which the decay rate $k \to 0$. In this case we are able to provide a simpler algorithmic solution as we state next.

Lemma IV.6 *Let* Q *be given by* (6) *and define its Schur complement*

$$\begin{aligned} R &\triangleq TB^E A - E - TB^I A(-D)^{-1}E \\ &= T(B^E A + B^I A D^{-1}E) - E, \end{aligned}$$

then Q *is Hurwitz if and only if* R *is Hurwitz.*

Proof: We begin by showing the sufficiency of the result. Since Q is Metzler, there exists $\phi > 0$ such that $Q + \phi I$ nonnegative. Furthermore, it is easy to see that Q is irreducible due to $A_{\mathcal{G}}$ being strongly connected.

Then, by [34, Theorem 2.2],

$$\begin{aligned} \rho(Q + \phi I) &= \lambda_1(Q) + \phi \\ &= \rho(TB^E A - E + \phi I - TB^I A(\rho(Q + \phi I)I - D)^{-1}E) \\ &< \rho(TB^E A - E + \phi I - TB^I A(-D)^{-1}E) = \lambda_1(R) + \phi, \end{aligned}$$

which is well defined because $-D$ is diagonal with strictly positive elements. Since the inequality is an almost direct result of [35, Lemma 3], we have omitted its proof. Thus, $\lambda_1(R) < 0$ implies $\lambda_1(Q) < 0$.

Necessity follows from a direct application of [34, Theorem 2.2].

■

Theorem IV.7 (Solution to eradication problem) *Assume the cost function* f *satisfies Assumption 1, and choose* $\overline{k} > 0$ *arbitrarily small. Then, Problem III.5 can be solved by solving the following auxiliary geometric program with decision variables* $\left\{\beta_i^I, \beta_i^E, \delta_i, \tau_i, u_i\right\}_{i=1}^N$

$$\begin{aligned} \text{min.} \quad & \textstyle\sum_{j=1}^N h_j^I\left(\beta_j^I\right) + h_j^E\left(\beta_j^E\right) + g_j\left(\delta_j\right) + \widetilde{f}_j\left(\tau_j\right) \\ \text{s.t.} \quad & \frac{\sum_{j=1}^N a_{ij}\tau_i u_j\left(\beta_i^E + \frac{\varepsilon_j}{\delta_j}\beta_i^I\right) + (\phi - \varepsilon_i)u_i}{\phi - \overline{k}} \leq u_i, \\ & \tfrac{\gamma_i}{\overline{\theta}_i + \gamma_i} \leq \tau_i \leq \tfrac{\gamma_i}{\underline{\theta}_i + \gamma_i}, \\ & \underline{\delta}_i \leq \delta_i \leq \overline{\delta}_i, \\ & \left(\underline{\beta}_i^I, \underline{\beta}_i^E\right) \leq \left(\beta_i^I, \beta_i^E\right) \leq \left(\overline{\beta}_i^I, \overline{\beta}_i^E\right), \end{aligned} \tag{16}$$

for all $i \in \{1, \dots, N\}$, *where* $\theta_i^* = \frac{\gamma_i(1-\tau_i^*)}{\tau_i^*}$ *solves the problem with cost*

$$C^* = \sum_{i=1}^{N} h_i^I(\beta_i^{I^*}) + h_i^E(\beta_i^{E^*}) + g_i(\delta_i^*) + f_i(\theta_i^*).$$

Proof: We begin by going back to the original definition of Q given in (6). To solve Problem III.5, we are only interested in ensuring that Q is Hurwitz. We now apply the same trick as before by creating a nonnegative matrix $\overline{R} = R + \phi \mathbf{I}$. Using Proposition IV.1 and the fact that $\lambda_1(\overline{R}) = \lambda_1(R) + \phi$, the proposed optimization ensures that $\lambda_1(R) \leq -\overline{k}$. This then ensures Q is Hurwitz as a result of Lemma IV.6. ■

Remark IV.8 For simplicity, we have considered $\varepsilon_i > 0$ as a fixed parameter for all nodes throughout this paper. However, design over this parameter can also be considered using the same methods proposed above. •

V. Simulations

Here we demonstrate the effectiveness of the algorithms proposed in Section IV-B through simulations on a randomly generated strongly connected digraph with $N = 20$ nodes. We begin by showing how the proposed optimization algorithms determine allocations to ensure the deterministic mean-field approximation (3) satisfies the desired properties. Comparisons are then made with the trajectories of the exact Markov process (1). The fixed parameters are randomly generated for each node with $\varepsilon_i \in [0.2, 0.4]$ and $\gamma_i \in [0.05, 0.45]$. For the decision variables we use the lower and upper bounds

$$\underline{\beta}_i^I = 0.05, \quad \overline{\beta}_i^I = 0.6, \quad \underline{\beta}_i^E = 0.1, \quad \overline{\beta}_i^E = 0.7,$$
$$\underline{\delta}_i = 0.1, \quad \overline{\delta}_i = 1, \quad \underline{\theta}_i = 0.1, \quad \overline{\theta}_i = 1,$$

for all nodes $i \in \{1, \ldots, N\}$. The cost functions associated with our decision variables are given by

$$h_i^I(\beta_i^I) = \tfrac{1}{\beta_i^I} - \tfrac{1}{\overline{\beta}_i^I}, \qquad h_i^E(\beta_i^E) = \tfrac{1}{\beta_i^E} - \tfrac{1}{\overline{\beta}_i^E},$$
$$g_i(\delta_i) = \tfrac{1}{\phi - \delta_i} - \tfrac{1}{\phi - \underline{\delta}_i}, \quad f_i(\theta_i) = \tfrac{\theta_i + \gamma_i}{\gamma_i} - \tfrac{\underline{\theta}_i + \gamma_i}{\gamma_i}.$$

Note that the preemptive cost functions h_i^I and h_i^E are monotonically decreasing functions while the preventative costs f_i and corrective costs g_i are monotonically increasing functions.

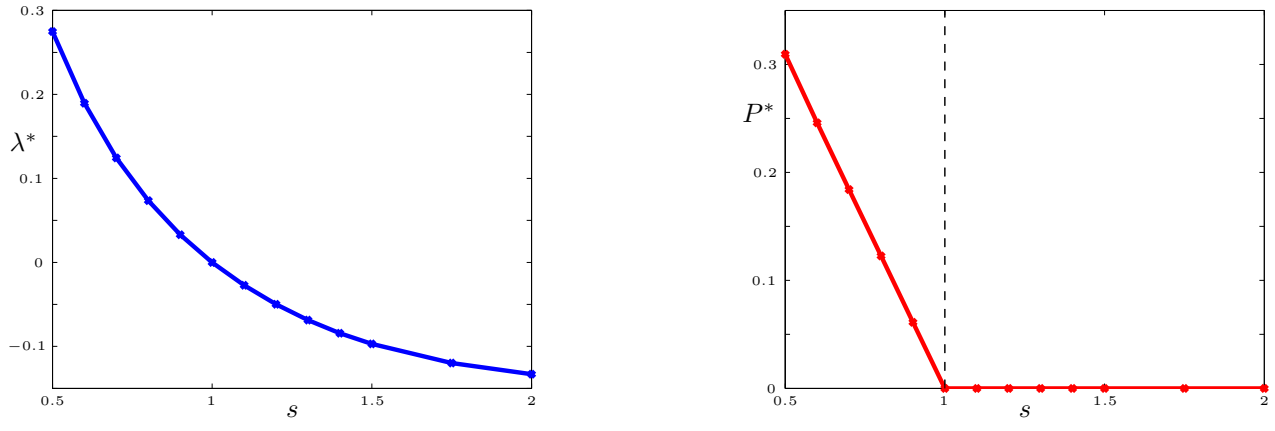

(a) (b)

Fig. 2. Plots of (a) the achieved decay rate $\lambda^* = \lambda_1(Q)$ and (b) the average steady state probabilities of infection $P^* = \frac{1}{N}\sum_{i=1}^N p_i^{E^*} + p_i^{I^*}$ for a budget of $C^* s$ where C^* is the optimal cost for ensuring eradication of the virus, i.e., $\lambda_1(Q) < 0$.

Fig. 2 demonstrates the performance achieved using the budget-constrained allocation algorithm from Theorem IV.3. We begin by solving the eradication problem posed in Problem III.5 to find the optimal cost C^* for eradicating the virus, i.e.,

$\lambda_1(Q) < 0$. We then allow a budget of C^*s where s is a scaling of this optimal cost to see how the algorithm performs. Fig. 2(a) shows the achieved decay rate $\lambda_1(Q)$ given the budget C^*s for varying values of s and Fig. 2(b) shows the steady state value of the average infection rate across all nodes $P^* = \frac{1}{N}\sum_{i=1}^{N} p_i^{E^*} + p_i^{I^*}$. As expected, we see that the virus can be fully eradicated for $s \geq 1$, which means we allow a budget greater than or equal to the minimum required cost. Conversely, for $s < 1$ the virus cannot be fully eradicated because the matrix Q cannot be made Hurwitz, which is consistent with the necessary and sufficient condition of Proposition III.1.

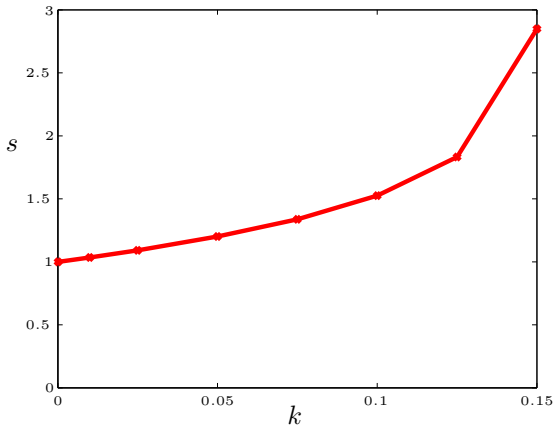

Fig. 3. Plot of the cost $C = C^*s$ required to achieve a desired decay rate $k > 0$ where C^* is the optimal cost for ensuring eradication of the virus, i.e., $\lambda_1(Q) < 0$.

Fig. 3 demonstrates the performance achieved using the rate-constrained allocation algorithm from Theorem IV.5. The plot shows the required cost $C = C^*s$ as a function of the desired decay rate $k > 0$. As expected, we see that as $k \to 0$ we recover the eradication problem and thus we have that $C \to C^*$.

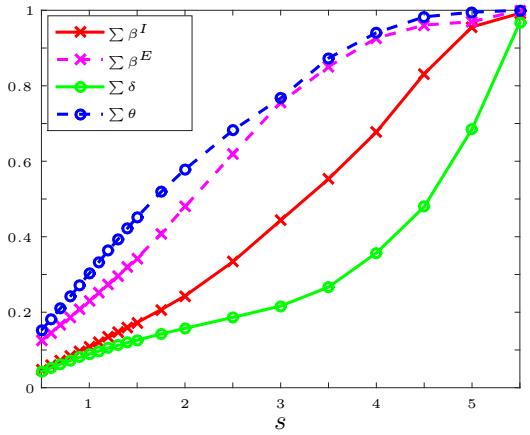

Fig. 4. Plots of the normalized amount of the corrective, preventative, and preemptive resources allocated for a budget of C^*s where C^* is the optimal cost for ensuring eradication of the virus, i.e., $\lambda_1(Q) < 0$.

Fig. 4 shows how the corrective, preventative, and preemptive resources are allocated as we increase the allowed budget. Interestingly, we see that corrective resources are the least important to be allocated in terms of containing an epidemic. This means that vaccinations and minimizing exposure to the disease is more important than deploying antidotes or cures.

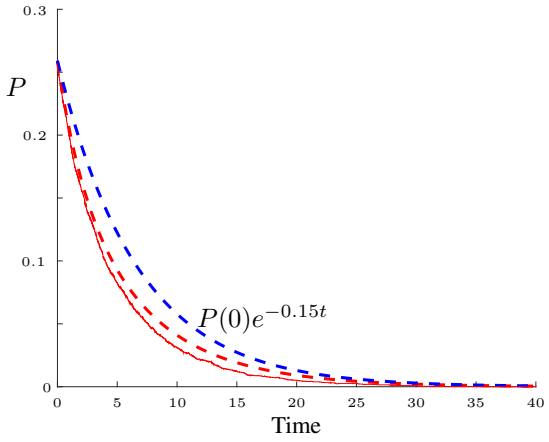

Fig. 5. Plots of the trajectories of $P(t) = \frac{1}{N}\sum_{i=1}^{N} p_i^E(t) + p_i^I(t)$ for the exact Markov process (solid red, average of 400 simulations) and the mean-field approximation (dashed red) with parameters obtained from Theorem IV.5 for $k = 0.15$. The dashed blue line shows the theoretical upper bound as given in (25).

Fig. 5 shows the trajectories of the average infection rate $P(t) = \frac{1}{N}\sum_{i=1}^{N} p_i^E(t) + p_i^I(t)$. The solid red line shows the average trajectories of the exact Markov process for 400 simulations and the dashed red line shows the trajectories of the deterministic mean-field approximation. This helps validate the claim that the mean-field approximation is an upper bound on the true expectation of infection in the stochastic model but this has yet to be shown. We also plot the theoretical upper bound provided in (25) for an achieved $\lambda_1(Q) \leq -0.15$ to show the effectiveness of controlling the maximum eigenvalue of Q.

VI. Conclusions

We have proposed the Generalized Susceptible-Exposed-Infected-Vigilant (G-SEIV) model for spreading processes on arbitrary networks. The G-SEIV model generalizes many existing models and also accounts for arbitrary directed graphs and heterogeneous node parameters. We have carefully analyzed the disease-free equilibrium and provided necessary and sufficient conditions for global exponential convergence to this equilibrium. Using this analysis, we have studied and shown how to solve two important optimal allocation problems. Provided with suitable cost functions for deploying corrective, preventative, or preemptive resources (e.g., antidotes, vaccines, awareness campaigns, or quarantining certain areas, in the context of a spreading disease), the first problem is finding the optimal cost for achieving a desired decay rate of the disease. The second problem is, given a fixed budget, finding the optimal allocation that achieves the maximum possible decay rate. We are able to efficiently solve these problems in polynomial time by reformulating them as quasiconvex optimization problems known as geometric programs. In the future, we are interested in formally showing that the infectious states of the deterministic mean-field approximation used upper-bounds the expectation of the original stochastic model proposed in this paper. We also plan to also provide analysis for the endemic equilibrium, i.e., the case where the disease-free equilibrium is not globally asymptotically stable. Future work on the control side will be devoted to cases in which parameters of the problem are unknown and we instead only have access to some empirical measurements of the evolution of the disease.

APPENDIX

Proof of Proposition III.1

In what follows, we begin by studying the local stability of the disease-free equilibrium via the Jacobian matrix of the system of ODEs in (5) evaluated at this equilibrium point. This analysis is easier to perform using a change of coordinates that translates the disease-free equilibrium to the origin. This translation can be achieved defining the following new variable:

$$r_i \triangleq p_i^V - \frac{\theta_i + (\delta_i - \theta_i)p_i^I - \theta_i p_i^E}{\theta_i + \gamma_i}. \tag{17}$$

Using this new variable, we can rewrite the system of ODEs in (5) as follows:

$$\begin{aligned}
\dot{p}_i^E &= \left(\frac{\gamma_i}{\theta_i+\gamma_i} - \frac{\gamma_i}{\theta_i+\gamma_i}p_i^E - \frac{\delta_i+\gamma_i}{\theta_i+\gamma_i}p_i^I - r_i\right)\sum_{j\in\mathcal{N}_i^{\text{in}}}(\beta_i^E p_j^E + \beta_i^I p_j^I) - \varepsilon_i p_i^E,\\
\dot{p}_i^I &= \varepsilon_i p_i^E - \delta_i p_i^I,\\
\dot{r}_i &= -\frac{\varepsilon_i\delta_i}{\theta_i+\gamma_i}p_i^E - \frac{\delta_i(\theta_i-\delta_i)}{\theta_i+\gamma_i}p_i^I - (\theta_i+\gamma_i)r_i + \frac{\theta_i\gamma_i}{(\theta_i+\gamma_i)^2}\sum_{j\in\mathcal{N}_i^{\text{in}}}(\beta_i^E p_j^E + \beta_i^I p_j^I)\\
&\quad - \frac{\theta_i}{\theta_i+\gamma_i}\Big[\Big(\frac{\gamma_i}{\theta_i+\gamma_i}p_i^E + \frac{\delta_i+\gamma_i}{\theta_i+\gamma_i}p_i^I + r_i\Big)\sum_{j\in\mathcal{N}_i^{\text{in}}}(\beta_i^E p_j^E + \beta_i^I p_j^I)\Big].
\end{aligned}$$

Although seemingly more complicated, this new system of equations allows for a simpler analysis of stability. We can rewrite the above system of ODEs in matrix-vector form by defining the following vector variables: $\mathbf{p}^E \triangleq (p_1^E, \ldots, p_N^E)^T$, $\mathbf{p}^I \triangleq (p_1^I, \ldots, p_N^I)^T$, and $\mathbf{r} \triangleq (r_1, \ldots, r_N)^T$. In the following, we use these vectors to express the dynamics of the spread in vector form, while separating the linear and nonlinear components of the dynamics, as follows:

$$\begin{bmatrix} \dot{\mathbf{p}}^E \\ \dot{\mathbf{p}}^I \\ \dot{\mathbf{r}} \end{bmatrix} = \mathcal{Q}\begin{bmatrix} \mathbf{p}^E \\ \mathbf{p}^I \\ \mathbf{r} \end{bmatrix} + \begin{bmatrix} H^E \\ 0 \\ H^r \end{bmatrix}, \tag{18}$$

where the matrix $\mathcal{Q}$, defined below, is associated with the linear part of the dynamics, and the nonlinear components are encapsulated in the vectors $H^E = (H_1^E, \ldots, H_N^E)$ and $H^r = (H_1^r, \ldots, H_N^r)$, with

$$H_i^E \triangleq -\Big(\frac{\gamma_i}{\theta_i+\gamma_i}p_i^E + \frac{\delta_i+\gamma_i}{\theta_i+\gamma_i}p_i^I + r_i\Big)\sum_{j\in\mathcal{N}_i^{\text{in}}}(\beta_i^E p_j^E + \beta_i^I p_j^I), \tag{19}$$

$$H_i^r \triangleq -\frac{\theta_i}{\theta_i+\gamma_i}\Big(\Big(\frac{\gamma_i}{\theta_i+\gamma_i}p_i^E + \frac{\delta_i+\gamma_i}{\theta_i+\gamma_i}p_i^I + r_i\Big)\sum_{j\in\mathcal{N}_i^{\text{in}}}(\beta_i^E p_j^E + \beta_i^I p_j^I)\Big). \tag{20}$$

In particular, the matrix $\mathcal{Q}$ in (18) is given by

$$\mathcal{Q} \triangleq \begin{bmatrix} TB^E A_{\mathcal{G}} - E & TB^I A_{\mathcal{G}} & 0 \\ E & -D & 0 \\ \mathcal{Q}_{31} & \mathcal{Q}_{32} & \mathcal{Q}_{33} \end{bmatrix}, \tag{21}$$

where

$$\begin{aligned}
\mathcal{Q}_{31} &\triangleq \operatorname{diag}\left(\frac{\theta\gamma}{(\theta+\gamma)^2}\beta^E\right)A_{\mathcal{G}} - \operatorname{diag}\left(\frac{\varepsilon\delta}{\theta+\gamma}\right),\\
\mathcal{Q}_{32} &\triangleq \operatorname{diag}\left(\frac{\theta\gamma}{(\theta+\gamma)^2}\beta^I\right)A_{\mathcal{G}} - \operatorname{diag}\left(\frac{\delta(\theta-\delta)}{\theta+\gamma}\right),\\
\mathcal{Q}_{33} &\triangleq -\operatorname{diag}(\theta+\gamma).
\end{aligned}$$

The nonlinear terms in (18), described in (19) and (20), can be written in terms of the original variable p_i^V using (17), as

$$H_i^E = -\left(p_i^E + p_i^I + p_i^V\right) \sum_{j \in \mathcal{N}_i^{\text{in}}} (\beta_i^E p_j^E + \beta_i^I p_j^I), \tag{22}$$

$$H_i^r = -\frac{\theta_i}{\theta_i + \gamma_i} \left(\left(p_i^E + p_i^I + p_i^V\right) \sum_{j \in \mathcal{N}_i^{\text{in}}} (\beta_i^E p_j^E + \beta_i^I p_j^I) \right). \tag{23}$$

Then, from (2) we see that $H_i^E, H_i^r \leq 0$ for all $i \in \{1, \ldots, N\}$ at all times. Letting $\mathbf{X} \triangleq [\mathbf{p}^E, \mathbf{p}^I, \mathbf{r}]$ and $H \triangleq [H^E, \mathbf{0}, H^r]$, this means that the linear system

$$\dot{\mathbf{X}} = \mathcal{Q}\mathbf{X} \tag{24}$$

upper bounds the original nonlinear system (18),

$$\mathcal{Q}\mathbf{X} + H \leq \mathcal{Q}\mathbf{X}. \tag{25}$$

Since the linear system (24) upper bounds the nonlinear dynamics (18), we are able to bound the rate of spreading of the nonlinear system by controlling the maximum eigenvalue of $\mathcal{Q}$. This provides a sufficient condition for global exponential convergence. Notice that, due to the structure of $\mathcal{Q}$ in (21), N of the eigenvalues of $\mathcal{Q}$ are equal to the eigenvalues of $\mathcal{Q}_{33}$, which are given by $-(\theta_i + \gamma_i)$ for $i = 1, \ldots, N$. The other $2N$ eigenvalues are equal to those of the $2N \times 2N$ matrix Q, defined in (6) as

$$Q = \begin{bmatrix} TB^E A_{\mathcal{G}} - E & TB^I A_{\mathcal{G}} \\ E & -D \end{bmatrix}.$$

In fact, the largest real part of the spectrum of Q determines the exponential rate in which the epidemics dies out. Necessity for global exponential convergence follows from [36, Theorem 4.15].

ACKNOWLEDGEMENTS

The authors would like to thank Prof. Francesco Bullo for pointing out the works [6] and [7]. This work was supported in part by NSF grants CNS-1302222 and IIS-1447470, and TerraSwarm, one of six centers of STARnet, a Semiconductor Research Corporation program sponsored by MARCO and DARPA.

REFERENCES

[1] C. Nowzari, V. M. Preciado, and G. J. Pappas, "Stability analysis of generalized epidemic models over directed networks," in *IEEE Conf. on Decision and Control*, Los Angeles, CA, Dec. 2014, pp. 6197–6202.

[2] N. T. Bailey, *The Mathematical Theory of Infectious Diseases and its Applications*. London: Griffin, 1975.

[3] M. M. Williamson and J. Leveille, "An epidemiological model of virus spread and cleanup," in *Virus Bulletin*, Toronto, Canada, 2003.

[4] M. Garetto, W. Gong, and D. Towsley, "Modeling malware spreading dynamics," in *INFOCOM Joint Conference of the IEEE Computer and Communications*, 2003, pp. 1869–1879.

[5] J. Leskovec, L. A. Adamic, and B. A. Huberman, "The dynamics of viral marketing," *ACM Transactions on the Web (TWEB)*, vol. 1, no. 1, 2007.

[6] A. Fall, A. Iggidr, G. Sallet, and J.-J. Tewa, "Epidemiological models and Lyapunov functions," *Mathematical Modelling of Natural Phenomena*, vol. 2, no. 1, pp. 62–68, 2007.

[7] A. Lajmanovich and J. A. Yorke, "A deterministic model for gonorrhea in a nonhomogeneous population," *Mathematical Biosciences*, vol. 28, no. 3, pp. 221–236, 1976.

[8] Y. Hu, H. Chen, J. Lou, and J. Li, "Epidemic spreading in real networks: An eigenvalue viewpoint," in *Proc. Symp. Reliable Distributed Systems*, 2003, pp. 25–34.

[9] P. V. Miegham, J. Omic, and R. Kooij, "Virus spread in networks," *IEEE/ACM Transactions on Networking*, vol. 17, no. 1, pp. 1–14, 2009.

[10] H. J. Ahn and B. Hassibi, "Global dynamics of epidemic spread over complex networks," in *IEEE Conf. on Decision and Control*, Florence, Italy, 2013, pp. 4579–4585.

[11] D. Easley and J. Kleinberg, *Networks, Crowds, and Markets: Reasoning About a Highly Connected World*. Cambridge, UK: Cambridge University Press, 2010.

[12] P. V. Mieghem and J. Omic, "In-homogeneous virus spread in networks," *arXiv preprint arXiv:1306.2588*, 2014.

[13] K. Drakopoulos, A. Ozdaglar, and J. N. Tsitsiklis, "An efficient curing policy for epidemics on graphs," *arXiv preprint arXiv:1407.2241*, 2014.

[14] A. Khanafer and T. Basar, "An optimal control problem over infected networks," in *Proceedings of the International Conference of Control, Dynamic Systems, and Robotics*, Ottawa, Ontario, Canada, 2014.

[15] Y. Wan, S. Roy, and A. Saberi, "Designing spatially heterogeneous strategies for control of virus spread," *Systems Biology, IET*, vol. 2, no. 4, pp. 184–201, 2008.

[16] V. M. Preciado, M. Zargham, C. Enyioha, A. Jadbabaie, and G. J. Pappas, "Optimal vaccine allocation to control epidemic outbreaks in arbitrary networks," in *IEEE Conf. on Decision and Control*, Florence, Italy, 2013, pp. 7486–7491.

[17] V. M. Preciado and M. Zargham, "Traffic optimization to control epidemic outbreaks in metapopulation models," in *IEEE Global Conference on Signal and Information Processing*, Austin, TX, 2013.

[18] E. Ramirez-Llanos and S. Martinez, "A distributed algorithm for virus spread minimization," in *American Control Conference*, Portland, OR, 2014, pp. 184–189.

[19] Y. Hayel, S. Trajanovski, E. Altman, H. Wang, and P. V. Mieghem, "Complete game-theoretic characterization of sis epidemics protection strategies," in *IEEE Conf. on Decision and Control*, Los Angeles, CA, 2014, pp. 1179–1184.

[20] X. Chen and V. M. Preciado, "Optimal coinfection control of competitive epidemics in multi-layer networks," in *IEEE Conf. on Decision and Control*, Los Angeles, CA, 2014, pp. 6209–6214.

[21] V. M. Preciado, M. Zargham, C. Enyioha, A. Jadbabaie, and G. J. Pappas, "Optimal resource allocation for network protection: A geometric programming approach," *IEEE Transactions on Networked Control Systems*, vol. 1, no. 1, pp. 99–108, 2014.

[22] F. D. Sahneh and C. Scoglio, "Epidemic spread in human networks," in *IEEE Conf. on Decision and Control*, Orlando, FL, 2011, pp. 3008–3013.

[23] V. M. Preciado, F. D. Sahneh, and C. Scoglio, "A convex framework for optimal investment on disease awareness in social networks," in *IEEE Global Conference on Signal and Information Processing*, Austin, TX, 2013.

[24] B. A. Prakash, D. Chakrabarti, M. Faloutsos, N. Valler, and C. Faloutsos, "Got the flu (or mumps)? check the eigenvalue!" *arXiv preprint arXiv:1004.0060*, 2010.

[25] H. W. Hethcote, "The mathematics of infectious diseases," *SIAM Review*, vol. 42, no. 4, pp. 599–653, 2000.

[26] P. V. Mieghem, *Performance Analysis of Communications Networks and Systems*. Cambridge, UK: Cambridge University Press, 2009.

[27] J. P. Gleeson, S. Melnik, J. A. Ward, M. A. Porter, and P. J. Mucha, "Accuracy of mean-field theory for dynamics on real-world networks," *Physical Review E*, vol. 85, p. 026106, 2012.

[28] P. V. Mieghem, "The n-intertwined SIS epidemic network model," *Computing*, vol. 93, no. 2-4, pp. 147–169, 2011.

[29] E. Cator and P. V. Mieghem, "Second-order mean-field susceptible-infected-susceptible epidemic threshold," *Physical Review E*, vol. 85, p. 056111, 2012.

[30] C. Li, R. van de Bovenkamp, and P. V. Mieghem, "Susceptible-infected-susceptible model: A comparison of n-intertwined and heterogeneous mean-field approximations," *Physical Review E*, vol. 86, p. 026116, 2012.

[31] N. A. Ruhi and B. Hassibi, "SIRS epidemics on complex networks: Concurrence of exact Markov chain and approximated models," *arXiv:1503.07576*, 2015.

[32] S. Boyd and L. Vandenberghe, *Convex Optimization*. Cambridge University Press, 2004.

[33] S. Boyd, S. J. Kim, L. Vandenberghe, and A. Hassibi, "A tutorial on geometric programming," *Optimization and Engineering*, vol. 8, no. 1, pp. 67–127, 2007.

[34] C. D. Meyer, "Uncoupling the Perron eigenvector problem," *Linear Algebra and its Applications*, vol. 114.

[35] LL:01, "Perron complement and Perron root," *Linear Algebra and its Applications*, vol. 341, pp. 239–248, 2001.

[36] H. K. Khalil, *Nonlinear Systems*, 3rd ed. Prentice Hall, 2002.